



HAL
open science

On the role of energy conservation in high-energy nuclear scattering

H.J. Drescher, M. Hladik, S. Ostapchenko, T. Pierog, Klaus Werner

► **To cite this version:**

H.J. Drescher, M. Hladik, S. Ostapchenko, T. Pierog, Klaus Werner. On the role of energy conservation in high-energy nuclear scattering. *New Journal of Physics*, 2000, 2, pp.31. 10.1088/1367-2630/2/1/331 . in2p3-00021456

HAL Id: in2p3-00021456

<https://hal.in2p3.fr/in2p3-00021456>

Submitted on 9 Jun 2007

HAL is a multi-disciplinary open access archive for the deposit and dissemination of scientific research documents, whether they are published or not. The documents may come from teaching and research institutions in France or abroad, or from public or private research centers.

L'archive ouverte pluridisciplinaire **HAL**, est destinée au dépôt et à la diffusion de documents scientifiques de niveau recherche, publiés ou non, émanant des établissements d'enseignement et de recherche français ou étrangers, des laboratoires publics ou privés.

On the role of energy conservation in high-energy nuclear scattering

H J Drescher¹, M Hladik^{1,3}, S Ostapchenko^{1,2}, T Pierog¹
and K Werner¹

¹ SUBATECH, Université de Nantes–IN2P3/CNRS–EMN, Nantes, France

² Moscow State University, Institute of Nuclear Physics, Moscow, Russia

E-mail: drescher@physics.nyu.edu

New Journal of Physics **2** (2000) 31.1–31.16 (<http://www.njp.org/>)

Received 26 June 2000; online 29 December 2000

Abstract. We argue that the most commonly used models for nuclear scattering at ultra-relativistic energies do not treat energy conservation in a consistent fashion. Demanding theoretical consistency as a minimal requirement for a realistic model, we provide a solution for the above-mentioned problem, the so-called ‘parton-based Gribov–Regge theory’.

In order to keep a clean picture, we do not consider secondary interactions. We provide a very transparent extrapolation of the physics of more elementary interactions towards nucleus–nucleus scattering, without considering any nuclear effects due to final state interactions. In this sense we consider our model a realistic and consistent approach to describe the initial stage of nuclear collisions.

1. Introduction

The purpose of this paper is to provide the theoretical framework to treat hadron–hadron scattering and the initial stage of nucleus–nucleus collisions at ultra-relativistic energies, in particular with view to RHIC (Relativistic Heavy Ion Collider) and LHC (Large Hadron Collider). The knowledge of these initial collisions is crucial for any theoretical treatment of parton thermalization and a possible parton–hadron phase transition, the detection of which being the ultimate aim of all the efforts of colliding heavy ions at very high energies.

Many popular models [1]–[3] are based on the so-called Gribov–Regge theory [4, 5]. This is an effective field theory, which allows multiple interactions to happen ‘in parallel’, with the phenomenological object called a ‘Pomeron’ representing an elementary interaction. Using the general rules of field theory, one may express cross sections in terms of a couple

³ Present address: SAP AG, Berlin, Germany.

of parameters characterizing the Pomeron. Interference terms are crucial, they assure the unitarity of the theory. Here one observes an *inconsistency*: the fact that energy needs to be shared between many Pomerons in the case of multiple scattering is well taken into account when calculating particle production (in particular in Monte Carlo applications), but energy conservation is not taken care of in cross section calculations. This is a serious problem and makes the whole approach inconsistent. Related to the above problem is the fact that different elementary interactions in the case of multiple scattering are usually not treated equally, so the first interaction is usually considered to be quite different compared to the subsequent interactions.

Provided factorization works for nuclear collisions, one may employ the parton model [6, 7], which allows to calculate inclusive cross sections as a convolution of an elementary cross section with parton distribution functions, with these distribution functions taken from deep inelastic scattering. In order to obtain exclusive parton level cross sections, some additional assumptions are needed, which follow quite closely the Gribov–Regge approach, encountering the same difficulties.

As a solution of the above-mentioned problems, we present a new approach which we call the ‘parton-based Gribov–Regge theory’: we have a consistent treatment for calculating cross sections and particle production considering energy conservation in both cases; in addition, we introduce hard processes in a natural way and, compared to the parton model, we can deal with exclusive cross sections without arbitrary assumptions. A single set of parameters is sufficient to fit many basic spectra in proton–proton and lepton–nucleon scattering, as well as in electron–positron annihilation (with the exception of one parameter which needs to be changed in order to optimize electron–positron transverse momentum spectra).

The basic guideline of our approach is theoretical consistency. We cannot derive everything from first principles, but we use rigorously the language of field theory to make sure not to violate basic laws of physics, which is easily done in more phenomenological treatments (see the discussion above).

There are still problems and open questions: there is clearly a problem with unitarity at very high energies, which should be cured by considering screening corrections due to so-called triple-Pomeron interactions, which we do not treat rigorously at present but which is our next project.

2. Problems

Before presenting new theoretical ideas, we want to discuss the open problems in the parton model approach and in the Gribov–Regge theory.

2.1. Gribov–Regge theory

The Gribov–Regge theory is by construction a multiple scattering theory. The elementary interactions are realized by complex objects called Pomerons, whose precise nature is not known, and which are therefore simply parametrized: the elastic amplitude T corresponding to a single Pomeron exchange is given as

$$T(s, t) \sim i s^{\alpha_0 + \alpha' t}$$

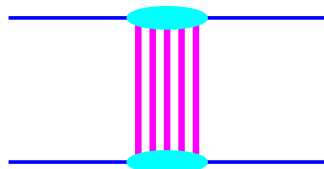


Figure 1. Hadron–hadron scattering in Gribov–Regge theory. The thick lines between the hadrons (incoming lines) each represent a Pomeron. The different Pomeron exchanges occur in parallel.

with a couple of parameters to be determined by experiment. Even in hadron–hadron scattering, several of these Pomerons are exchanged in parallel, see figure 1. Using general rules of field theory (cutting rules), one obtains an expression for the inelastic cross section,

$$\sigma_{\text{inel}}^{h_1 h_2} = \int d^2b \{1 - \exp(-G(s, b))\} \quad (1)$$

where the so-called eikonal $G(s, b)$ (proportional to the Fourier transform of $T(s, t)$) represents one elementary interaction (a vertical thick line in figure 1). One can generalize to nucleus–nucleus collisions, where corresponding formulae for cross sections may be derived.

In order to calculate exclusive particle production, one needs to know how to share the energy between the individual elementary interactions in the case of multiple scattering. We do not want to discuss the different recipes used to perform the energy sharing (in particular in Monte Carlo applications). The point is, whatever procedure is used this is not taken into account in the calculation of cross sections discussed above. So, in actually, one is using two different models for cross section calculations and for treating particle production. Taking energy conservation into account in exactly the same way will considerably modify the cross section results.

This problem was first discussed in [8, 9]. The authors claim that following from the non-planar structure of the corresponding diagrams, conserving energy and momentum in a consistent way is crucial, and therefore the incident energy has to be shared between the different elementary interactions, both real and virtual interactions.

Another very unpleasant and unsatisfactory feature of most ‘recipes’ for particle production is the fact that the second and subsequent Pomerons are treated differently from the first; although in the above-mentioned formula for the cross section all Pomerons are considered to be identical.

2.2. The parton model

The standard parton model approach to hadron–hadron or, also, nucleus–nucleus scattering amounts to presenting the partons of projectile and target by momentum distribution functions, f_{h_1} and f_{h_2} , and calculating inclusive cross sections for the production of parton jets with the squared transverse momentum p_{\perp}^2 larger than some cutoff Q_0^2 as

$$\sigma_{\text{incl}}^{h_1 h_2} = \sum_{ij} \int dp_{\perp}^2 \int dx^+ \int dx^- f_{h_1}^i(x^+, p_{\perp}^2) f_{h_2}^j(x^-, p_{\perp}^2) \frac{d\hat{\sigma}_{ij}}{dp_{\perp}^2}(x^+ x^- s) \theta(p_{\perp}^2 - Q_0^2)$$

where $d\hat{\sigma}_{ij}/dp_{\perp}^2$ is the elementary parton–parton cross section and i, j represent parton flavours.

This simple factorization formula is the result of cancellations of complicated diagrams (AGK cancellations) due to which only a single scattering term (one Pomeron exchange) contributes to the inclusive hadron spectra [20]. It hides, therefore, the complicated multiple

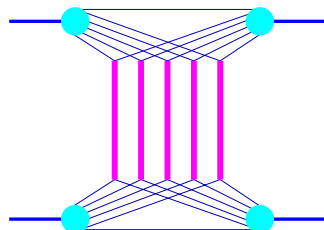


Figure 2. Graphical representation of a contribution to the elastic amplitude of proton–proton scattering. Here, energy conservation is taken into account: the energy of the incoming protons is shared among several ‘constituents’ (shown by splitting the nucleon lines into several constituent lines), and so each Pomeron disposes of only a fraction of the total energy, such that the total energy is conserved.

scattering structure of the reaction. The most obvious manifestation of such a structure is the fact that at high energies ($\sqrt{s} \gg 10$ GeV) the inclusive cross section in proton–(anti-)proton scattering exceeds the total one, so the average number $\bar{N}_{\text{int}}^{pp}$ of elementary interactions must be greater than one:

$$\bar{N}_{\text{int}}^{h_1 h_2} = \sigma_{\text{incl}}^{h_1 h_2} / \sigma_{\text{tot}}^{h_1 h_2} > 1.$$

The usual solution is the so-called eikonalization, which amounts to re-introducing multiple scattering, based on the above formula for the inclusive cross section:

$$\sigma_{\text{incl}}^{h_1 h_2}(s) = \int d^2b \{1 - \exp(-A(b)\sigma_{\text{incl}}^{h_1 h_2}(s))\} = \sum \sigma_m^{h_1 h_2}(s) \quad (2)$$

with

$$\sigma_m^{h_1 h_2}(s) = \int d^2b \frac{(A(b)\sigma_{\text{incl}}^{h_1 h_2}(s))^m}{m!} \exp(-A(b)\sigma_{\text{incl}}^{h_1 h_2}(s)) \quad (3)$$

representing the cross section for n scatterings. Here $A(b)$ is the proton–proton overlap function (the convolution of two proton profiles). In this way the multiple scattering is ‘recovered’. The disadvantage is that this method does not provide any clue how to proceed for nucleus–nucleus (AB) collisions. One usually assumes the proton–proton cross section for each individual nucleon–nucleon pair of an AB system. We can demonstrate that this assumption is incorrect (see [10]).

Another problem, in fact the same as discussed earlier for the Gribov–Regge theory, arises in the case of exclusive calculations (event generation), since the above formulae do not provide any information on how to share the energy between many elementary interactions. The Pythia method [6] amounts to generating the first elementary interaction according to the inclusive differential cross section, then taking the remaining energy for the second one and so on. In this way, the event generation will reproduce the theoretical inclusive spectrum for hadron–hadron interaction (by construction), as it should be. The method is, however, very arbitrary, and—even more serious—we observe the same inconsistency as in the Gribov–Regge approach: energy conservation is not at all taken care of in the above formulae for cross section calculations.

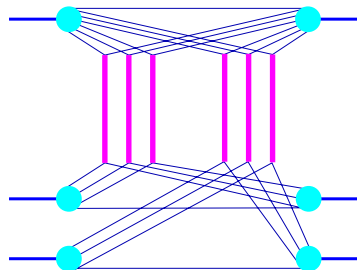


Figure 3. Graphical representation of a contribution to the elastic amplitude of proton–nucleus scattering, or more precisely a proton interacting with (for simplicity) two target nucleons, taking into account energy conservation. Here the energy of the incoming proton is shared between all the constituents, which now provide the energy to interact with two target nucleons.

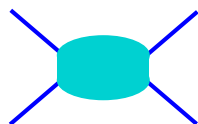


Figure 4. The soft contribution.

3. A solution: parton-based Gribov–Regge theory

In this paper, we present a new approach for hadronic interactions and for the initial stage of nuclear collisions, which is able to solve several of the above-mentioned problems. We provide a rigorous treatment of the multiple scattering aspect, such that questions as energy conservation are clearly determined by the rules of field theory, both for cross section and particle production calculations. In *both* cases, energy is properly shared between the different interactions occurring in parallel, see figure 2 for proton–proton and figure 3 for proton–nucleus collisions (generalization to nucleus–nucleus is obvious). This is the most important and new aspect of our approach, which we consider to be a first necessary step to take to construct a consistent model for high-energy nuclear scattering.

The elementary interactions, shown as the thick lines in the above figures, are in fact a sum of a soft, a hard and a semi-hard contribution, providing a consistent treatment of soft and hard scattering. To some extent, our approach provides a link between the Gribov–Regge approach and the parton model, we call it the parton-based Gribov–Regge theory.

4. Parton–parton scattering

Let us first investigate parton–parton scattering before constructing a multiple scattering theory for hadronic and nuclear scattering.

We distinguish three types of elementary parton–parton scatterings, referred to as ‘soft’, ‘hard’ and ‘semi-hard’, which we are going to discuss briefly in the following. The detailed derivations can be found in [10].

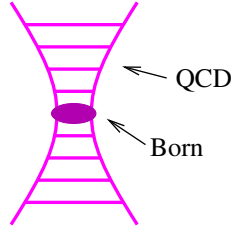


Figure 5. The hard (or valence–valence) contribution.

4.1. The soft contribution

Let us first consider a pure non-perturbative contribution, where all virtual partons appearing in the internal structure of the diagram have restricted virtualities $Q^2 < Q_0^2$, where $Q_0^2 \simeq 1 \text{ GeV}^2$ is a reasonable cutoff for perturbative quantum chromodynamics (QCD) being applicable. Such soft non-perturbative dynamics is known to dominate hadron–hadron interactions at not too high energies. Lacking methods to calculate this contribution from first principles, it is simply parametrized and graphically represented as a ‘blob’, see figure 4. It is traditionally assumed to correspond to multi-peripheral production of partons (and final hadrons) [11] and is described by the phenomenological soft Pomeron exchange amplitude $T_{\text{soft}}(\hat{s}, t)$ [4]. The corresponding profile function is expressed via the amplitude T_{soft} as

$$\begin{aligned} D_{\text{soft}}(\hat{s}, b) &= \frac{1}{8\pi^2 \hat{s}} \int d^2 q_{\perp} \exp(-i\vec{q}_{\perp} \vec{b}) 2 \text{Im} T_{\text{soft}}(\hat{s}, -q_{\perp}^2) \\ &= \frac{2\gamma_{\text{part}}^2}{\lambda_{\text{soft}}^{(2)}(\hat{s}/s_0)} \left(\frac{\hat{s}}{s_0}\right)^{\alpha_{\text{soft}}(0)-1} \exp\left(-\frac{b^2}{4\lambda_{\text{soft}}^{(2)}(\hat{s}/s_0)}\right) \end{aligned} \quad (4)$$

with

$$\lambda_{\text{soft}}^{(n)}(z) = nR_{\text{part}}^2 + \alpha'_{\text{soft}} \ln z$$

where \hat{s} is the usual Mandelstam variable for parton–parton scattering. The parameters $\alpha_{\text{soft}}(0)$ and α'_{soft} are the intercept and the slope of the Pomeron trajectory, γ_{part} and R_{part}^2 are the vertex value and the slope for the Pomeron–parton coupling and $s_0 \simeq 1 \text{ GeV}^2$ is the characteristic hadronic mass scale. The external legs of figure 4 are the ‘partonic constituents’, which are assumed to be quark–anti-quark pairs.

4.2. The hard contribution

Let us now consider the other extreme, when all the processes are perturbative, i.e. all internal intermediate partons are characterized by large virtualities $Q^2 > Q_0^2$. In such a case, the corresponding hard parton–parton scattering amplitude can be calculated using perturbative QCD techniques [12, 13], and the intermediate states contributing to the absorptive part of the amplitude can be defined in the parton basis. In the leading logarithmic approximation of QCD, summing up terms where each (small) running QCD coupling constant $\alpha_s(Q^2)$ appears together with a large logarithm $\ln(Q^2/\lambda_{\text{QCD}}^2)$ (with λ_{QCD} being the infrared QCD scale), and making use of the factorization hypothesis, one obtains the contribution of the corresponding cut diagram for $t = q^2 = 0$ as the cut parton ladder cross section $\sigma_{\text{hard}}^{jk}(\hat{s}, Q_0^2)$ ⁴, as shown in figure 5, where

⁴ Strictly speaking, one obtains the ladder representation for the process only by using an axial gauge.

all horizontal rungs are the final (on-shell) partons and the virtualities of the virtual t -channel partons increase from the ends of the ladder towards the largest momentum transfer parton–parton process (indicated symbolically by the ‘blob’ in the middle of the ladder):

$$\begin{aligned}\sigma_{\text{hard}}^{jk}(\hat{s}, Q_0^2) &= \frac{1}{2\hat{s}} 2 \text{Im} T_{\text{hard}}^{jk}(\hat{s}, t=0, Q_0^2) \\ &= K \sum_{ml} \int dx_B^+ dx_B^- dp_{\perp}^2 \frac{d\sigma_{\text{Born}}^{ml}}{dp_{\perp}^2}(x_B^+ x_B^- \hat{s}, p_{\perp}^2) \\ &\quad \times E_{\text{QCD}}^{jm}(Q_0^2, M_F^2, x_B^+) E_{\text{QCD}}^{kl}(Q_0^2, M_F^2, x_B^-) \theta(M_F^2 - Q_0^2).\end{aligned}$$

Here $d\sigma_{\text{Born}}^{ml}/dp_{\perp}^2$ is the differential $2 \rightarrow 2$ parton scattering cross section, p_{\perp}^2 is the parton transverse momentum in the hard process, m, l and x_B^{\pm} are respectively the types and the shares of the light cone momenta of the partons participating in the hard process; and M_F^2 is the factorization scale for the process (we use $M_F^2 = p_{\perp}^2/4$). The ‘evolution function’ $E_{\text{QCD}}^{jm}(Q_0^2, M_F^2, z)$ represents the evolution of a parton cascade from scale Q_0^2 to M_F^2 ; i.e. it gives the number density of partons of type m with the momentum share z at the virtuality scale M_F^2 as a result of the evolution of the initial parton j and taken at the virtuality scale Q_0^2 . The evolution function satisfies the usual DGLAP equation [14] with the initial condition $E_{\text{QCD}}^{jm}(Q_0^2, Q_0^2, z) = \delta_m^j \delta(1-z)$. The factor $K \simeq 1.5$ effectively takes into account higher-order QCD corrections.

In the following we shall need to know the contribution of the uncut parton ladder $T_{\text{hard}}^{jk}(\hat{s}, t, Q_0^2)$ with some momentum transfer q along the ladder (with $t = q^2$). The behaviour of the corresponding amplitudes was studied in [15] in the leading logarithmic ($1/x$) approximation of QCD. The precise form of the corresponding amplitude is not important for our application; we just use some of the results of [15], namely one can neglect the real part of this amplitude and it is nearly independent of t . That is the slope of the hard interaction R_{hard}^2 is negligibly small, i.e. compared to the soft Pomeron slope one has $R_{\text{hard}}^2 \simeq 0$. So we parametrize $T_{\text{hard}}^{jk}(\hat{s}, t, Q_0^2)$ in the region of small t as [16]

$$T_{\text{hard}}^{jk}(\hat{s}, t, Q_0^2) = i\hat{s} \sigma_{\text{hard}}^{jk}(\hat{s}, Q_0^2) \exp(R_{\text{hard}}^2 t). \quad (5)$$

The corresponding profile function is obtained by calculating the Fourier transform $\tilde{T}_{\text{hard}}^{jk}$ of T_{hard}^{jk} and dividing by the initial parton flux $2\hat{s}$,

$$D_{\text{hard}}^{jk}(\hat{s}, b) = \frac{1}{2\hat{s}} 2 \text{Im} \tilde{T}_{\text{hard}}^{jk}(\hat{s}, b)$$

which gives

$$\begin{aligned}D_{\text{hard}}^{jk}(\hat{s}, b) &= \frac{1}{8\pi^2 \hat{s}} \int d^2 q_{\perp} \exp(-i\vec{q}_{\perp} \vec{b}) 2 \text{Im} T_{\text{hard}}^{jk}(\hat{s}, -q_{\perp}^2, Q_0^2) \\ &= \sigma_{\text{hard}}^{jk}(\hat{s}, Q_0^2) \frac{1}{4\pi R_{\text{hard}}^2} \exp\left(-\frac{b^2}{4R_{\text{hard}}^2}\right).\end{aligned} \quad (6)$$

In fact, the above considerations are only correct for valence quarks, as discussed in detail in the next section. Therefore, we also talk about a ‘valence–valence’ contribution and we use $D_{\text{val–val}}$ instead of D_{hard} :

$$D_{\text{val–val}}^{jk}(\hat{s}, b) \equiv D_{\text{hard}}^{jk}(\hat{s}, b)$$

so these are two names for one and the same object.

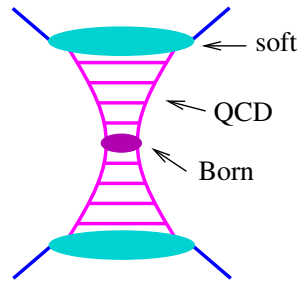


Figure 6. The semi-hard ‘sea–sea’ contribution: parton ladder plus ‘soft ends’.

4.3. The semi-hard contribution

The discussion of the preceding section is not valid in case of sea quarks and gluons, since here the momentum share x_1 of the ‘first’ parton is typically very small, leading to an object with a large mass of the order Q_0^2/x_1 between the parton and the proton [17]. Microscopically, such ‘slow’ partons with $x_1 \ll 1$ appear as a result of a long non-perturbative parton cascade, where each individual parton branching is characterized by a small momentum transfer squared $Q^2 < Q_0^2$ [4, 18]. When calculating proton structure functions or high- p_t jet production cross sections this non-perturbative contribution is usually included in parametrized initial parton momentum distributions at $Q^2 = Q_0^2$. However, the description of inelastic hadronic interactions requires one to treat it explicitly in order to account for secondary particles produced during such non-perturbative parton pre-evolution, and to describe correctly energy-momentum sharing between multiple elementary scatterings. As the underlying dynamics appears to be identical to that of soft parton–parton scattering considered above, we treat this soft pre-evolution as the usual soft Pomeron emission, as discussed in detail in [10].

So for sea quarks and gluons we consider so-called semi-hard interactions between parton constituents of initial hadrons, represented by a parton ladder with ‘soft ends’, see figure 6. As in the case of soft scattering, the external legs are quark-anti-quark pairs, connected to soft Pomerons. The outer partons of the ladder are sea quarks or gluons on both sides (therefore the index ‘sea–sea’). The central part is exactly the hard scattering considered in the preceding section. As discussed at length in [10], the mathematical expression for the corresponding amplitude is given as

$$iT_{\text{sea-sea}}(\hat{s}, t) = \sum_{jk} \int_0^1 \frac{dz^+}{z^+} \frac{dz^-}{z^-} \text{Im} T_{\text{soft}}^j \left(\frac{s_0}{z^+}, t \right) \text{Im} T_{\text{soft}}^k \left(\frac{s_0}{z^-}, t \right) iT_{\text{hard}}^{jk}(z^+ z^- \hat{s}, t, Q_0^2)$$

with z^\pm being the momentum fraction of the external leg partons of the parton ladder relative to the momenta of the initial (constituent) partons. The indices j and k refer to the flavour of these external ladder partons. The amplitudes T_{soft}^j are the soft Pomeron amplitudes discussed earlier, but with modified couplings, since the Pomerons are now connected to a parton ladder on one side. The arguments s_0/z^\pm are the squared masses of the two soft Pomerons, $z^+ z^- \hat{s}$ is the squared mass of the hard piece.

Performing, as usual, the Fourier transform to the impact parameter representation and dividing by $2\hat{s}$, we obtain the profile function

$$D_{\text{sea-sea}}(\hat{s}, b) = \frac{1}{2\hat{s}} 2 \text{Im} \tilde{T}_{\text{sea-sea}}(\hat{s}, b)$$

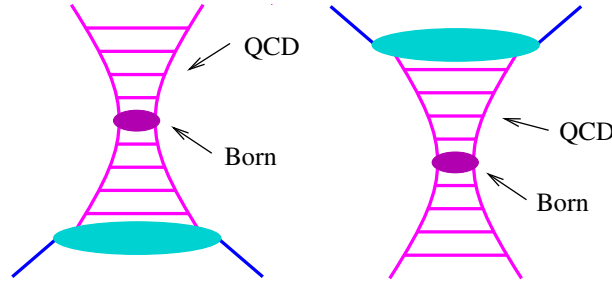


Figure 7. Two ‘mixed’ contributions.

which may be written as

$$D_{\text{sea-sea}}(\hat{s}, b) = \sum_{jk} \int_0^1 dz^+ dz^- E_{\text{soft}}^j(z^+) E_{\text{soft}}^k(z^-) \sigma_{\text{hard}}^{jk}(z^+ z^- \hat{s}, Q_0^2) \times \frac{1}{4\pi \lambda_{\text{soft}}^{(2)}(1/(z^+ z^-))} \exp\left(-\frac{b^2}{4\lambda_{\text{soft}}^{(2)}(1/(z^+ z^-))}\right) \quad (7)$$

with the soft Pomeron slope $\lambda_{\text{soft}}^{(2)}$ and the cross section $\sigma_{\text{hard}}^{jk}$ being defined earlier. The functions $E_{\text{soft}}^j(z^\pm)$ representing the ‘soft ends’ are defined as

$$E_{\text{soft}}^j(z^\pm) = \text{Im} T_{\text{soft}}^j\left(\frac{s_0}{z^\pm}, t = 0\right).$$

We neglected the small hard scattering slope R_{hard}^2 compared to the Pomeron slope $\lambda_{\text{soft}}^{(2)}$. We also call E_{soft} the ‘soft evolution’, to indicate that we consider this as simply a continuation of the QCD evolution in a region where perturbative techniques no longer apply. As discussed in [10], $E_{\text{soft}}^j(z)$ has the meaning of the momentum distribution of parton j in the soft Pomeron.

Consistency requires us to also consider the mixed semi-hard contributions with a valence quark on one side and a non-valence participant (quark–anti-quark pair) on the other, see figure 7. We have

$$iT_{\text{val-sea}}^j(\hat{s}) = \int_0^1 \frac{dz^-}{z^-} \sum_k \text{Im} T_{\text{soft}}^k\left(\frac{s_0}{z^-}, q^2\right) iT_{\text{hard}}^{jk}(z^- \hat{s}, q^2, Q_0^2)$$

and

$$D_{\text{val-sea}}^j(\hat{s}, b) = \sum_k \int_0^1 dz^- E_{\text{soft}}^k(z^-) \sigma_{\text{hard}}^{jk}(z^- \hat{s}, Q_0^2) \frac{1}{4\pi \lambda_{\text{soft}}^{(1)}(1/z^-)} \exp\left(-\frac{b^2}{4\lambda_{\text{soft}}^{(1)}(1/z^-)}\right) \quad (8)$$

where j is the flavour of the valence quark at the upper end of the ladder and k is the type of the parton on the lower ladder end. Again, we neglected the hard scattering slope R_{hard}^2 compared to the soft Pomeron slope. A contribution $D_{\text{sea-val}}^j(\hat{s}, b)$, corresponding to a valence quark participant from the target hadron, is given by the same expression,

$$D_{\text{sea-val}}^j(\hat{s}, b) = D_{\text{val-sea}}^j(\hat{s}, b)$$

since equation (8) stays unchanged under the replacement $z^- \rightarrow z^+$ and only depends on the total energy squared \hat{s} for the parton–parton centre-of-mass system.

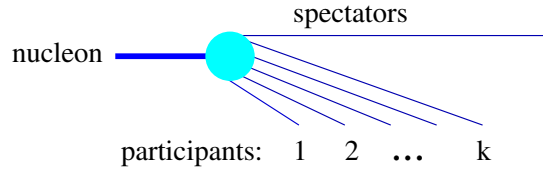


Figure 8. Nucleon Fock state.

5. Hadron–hadron scattering

To treat hadron–hadron scattering we use the parton momentum Fock state expansion of hadron eigenstates [8]

$$|h\rangle = \sum_{k=1}^{\infty} \frac{1}{k!} \int_0^1 \prod_{l=1}^k dx_l f_k^h(x_1, \dots, x_k) \delta\left(1 - \sum_{j=1}^k x_j\right) a^+(x_1) \cdots a^+(x_k) |0\rangle$$

where $f_k(x_1, \dots, x_k)$ is the probability amplitude for the hadron h to consist of k constituent partons with the light cone momentum fractions x_1, \dots, x_k and $a^+(x)$ is the creation operator for a parton with the fraction x . A general scattering process is described as a superposition of a number of pair-like scatterings between parton constituents of the projectile and target hadrons. Then the hadron–hadron scattering amplitude is obtained as a convolution of the individual parton–parton scattering amplitudes considered in the previous section and ‘inclusive’ momentum distributions $\frac{1}{n!} \tilde{F}_h^{(n)}(x_1, \dots, x_n)$ of n ‘participating’ parton constituents involved in the scattering process ($n \geq 1$), with

$$\frac{1}{n!} \tilde{F}_h^{(n)}(x_1, \dots, x_n) = \sum_{k=n}^{\infty} \frac{1}{k!} \frac{k!}{n!(k-n)!} \int_0^1 \prod_{l=n+1}^k dx_l |f_k(x_1, \dots, x_k)|^2 \delta\left(1 - \sum_{j=1}^k x_j\right).$$

We assume that $\tilde{F}_{h_1(h_2)}^{(n)}(x_1, \dots, x_n)$ can be represented in a factorized form as a product of the contributions of $F_{\text{part}}^h(x_l)$, depending on the momentum shares x_l of the ‘participating’ or ‘active’ parton constituents, and on the function $F_{\text{remn}}^h\left(1 - \sum_{j=1}^n x_j\right)$, representing the contribution of all ‘spectator’ partons that share the remaining share $1 - \sum_j x_j$ of the initial light cone momentum (see figure 8):

$$\tilde{F}_h^{(n)}(x_1, \dots, x_n) = \prod_{l=1}^n F_{\text{part}}^h(x_l) F_{\text{remn}}^h\left(1 - \sum_{j=1}^n x_j\right). \quad (9)$$

The participating parton constituents are assumed to be quark–anti-quark pairs (not necessarily of identical flavours), such that the baryon numbers of the projectile and of the target are conserved. Then, as discussed in detail in [10], the hadron–hadron amplitude may be written as

$$i T_{h_1 h_2}(s, t) = 8\pi^2 s \sum_{n=1}^{\infty} \frac{1}{n!} \int_0^1 \prod_{l=1}^n dx_l^+ dx_l^- \prod_{l=1}^n \left(\frac{1}{8\pi^2 \hat{s}_l} \int d^2 q_{l\perp} i T_{1P}^{h_1 h_2}(x_l^+, x_l^-, s, -q_{l\perp}^2) \right) F_{\text{remn}}^{h_1} \left(1 - \sum_{j=1}^n x_j^+\right) F_{\text{remn}}^{h_2} \left(1 - \sum_{j=1}^n x_j^-\right) \delta^{(2)} \left(\sum_{k=1}^n \vec{q}_{k\perp} - \vec{q}_{\perp} \right) \quad (10)$$

where the partonic amplitudes are defined as

$$T_{1P}^{h_1 h_2} = T_{\text{soft}}^{h_1 h_2} + T_{\text{sea-sea}}^{h_1 h_2} + T_{\text{val-val}}^{h_1 h_2} + T_{\text{val-sea}}^{h_1 h_2} + T_{\text{sea-val}}^{h_1 h_2}$$

with the individual contributions representing the ‘elementary partonic interactions plus external legs’. The soft or semi-hard sea–sea contributions are given as

$$T_{\text{soft/sea-sea}}^{h_1 h_2}(x^+, x^-, s, -q_\perp^2) = T_{\text{soft/sea-sea}}(s, -q_\perp^2) F_{\text{part}}^{h_1}(x^+) F_{\text{part}}^{h_2}(x^-) \exp(-[R_{h_1}^2 + R_{h_2}^2] q_\perp^2) \quad (11)$$

the hard contribution is

$$T_{\text{val-val}}^{h_1 h_2}(x^+, x^-, s, q^2) = \int_0^{x^+} dx_v^+ \frac{x^+}{x_v^+} \int_0^{x^-} dx_v^- \frac{x^-}{x_v^-} \sum_{j,k} T_{\text{hard}}^{jk}(x_v^+ x_v^- s, q^2, Q_0^2) \\ \times \bar{F}_{\text{part}}^{h_1, j}(x_v^+, x^+ - x_v^+) \bar{F}_{\text{part}}^{h_2, k}(x_v^-, x^- - x_v^-) \exp(-[R_{h_1}^2 + R_{h_2}^2] q_\perp^2)$$

the mixed semi-hard ‘val–sea’ contribution is given as

$$T_{\text{val-sea}}^{h_1 h_2}(x^+, x^-, s, q^2) = \int_0^{x^+} dx_v^+ \frac{x^+}{x_v^+} \sum_j T_{\text{val-sea}}^j(x_v^+ x^- s, q^2, Q_0^2) \\ \times \bar{F}_{\text{part}}^{h_1, j}(x_v^+, x^+ - x_v^+) F_{\text{part}}^{h_2}(x^-) \exp(-[R_{h_1}^2 + R_{h_2}^2] q_\perp^2)$$

and the contribution ‘sea–val’ is finally obtained from ‘val–sea’ by exchanging variables

$$T_{\text{sea-val}}^{h_1 h_2}(x^+, x^-, s, q^2) = T_{\text{val-sea}}^{h_2 h_1}(x^-, x^+, s, q^2).$$

Here we formally allow any number of valence type interactions (based on the fact that multiple valence type processes give negligible contributions). In the valence contributions, we have convolutions of hard parton scattering amplitudes T_{hard}^{jk} and valence quark distributions \bar{F}_{part}^j over the valence quark momentum share x_v^\pm rather than a simple product, since only the valence quarks are involved in the interactions, with the anti-quarks staying idle (the external legs carrying momenta x^+ and x^- are always quark–anti-quark pairs).

The profile function γ is as usual defined as

$$\gamma_{h_1 h_2}(s, b) = \frac{1}{2s} 2 \text{Im} \tilde{T}_{h_1 h_2}(s, b)$$

which may be evaluated using the AGK cutting rules with the result (assuming imaginary amplitudes)

$$\gamma_{h_1 h_2}(s, b) = \sum_{m=1}^{\infty} \frac{1}{m!} \int_0^1 \prod_{\mu=1}^m dx_\mu^+ dx_\mu^- \prod_{\mu=1}^m G_{1\text{P}}^{h_1 h_2}(x_\mu^+, x_\mu^-, s, b) \sum_{l=0}^{\infty} \frac{1}{l!} \int_0^1 \prod_{\lambda=1}^l d\tilde{x}_\lambda^+ d\tilde{x}_\lambda^- \\ \times \prod_{\lambda=1}^l -G_{1\text{P}}^{h_1 h_2}(\tilde{x}_\lambda^+, \tilde{x}_\lambda^-, s, b) F_{\text{remn}}\left(x^{\text{proj}} - \sum_{\lambda} \tilde{x}_\lambda^+\right) F_{\text{remn}}\left(x^{\text{targ}} - \sum_{\lambda} \tilde{x}_\lambda^-\right) \quad (12)$$

with $x^{\text{proj/targ}} = 1 - \sum x_\mu^\pm$ being the momentum fraction of the projectile/target remnant, and with a partonic profile function G given as

$$G_{1\text{P}}^{h_1 h_2}(x_\lambda^+, x_\lambda^-, s, b) = \frac{1}{2s} 2 \text{Im} \tilde{T}_{1\text{P}}^{h_1 h_2}(x_\lambda^+, x_\lambda^-, s, b) \quad (13)$$

see figure 9. This is a very important result, allowing one to express the total profile function $\gamma_{h_1 h_2}$ via the elementary profile functions $G_{1\text{P}}^{h_1 h_2}$.

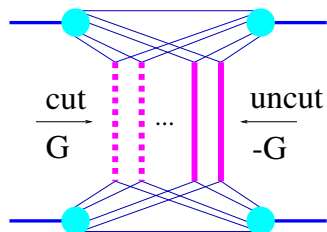


Figure 9. The hadronic profile function γ expressed in terms of partonic profile functions $G \equiv G_{1\mathbb{P}}^{h_1 h_2}$.

6. Nucleus–nucleus scattering

We generalize the discussion of the last section in order to treat nucleus–nucleus scattering. In the Glauber–Gribov approach [5, 19], the nucleus–nucleus scattering amplitude is defined by the sum of contributions of diagrams corresponding to multiple scattering processes between parton constituents of projectile and target nucleons. Nuclear form factors are supposed to be defined by the nuclear ground-state wavefunctions. Assuming the nucleons to be uncorrelated, one can make the Fourier transform to obtain the amplitude in the impact parameter representation. Then, for given impact parameter \vec{b}_0 between the nuclei, the only formal difference from the hadron–hadron case will be the averaging over the nuclear ground states, which amounts to an integration over the transverse nucleon coordinates \vec{b}_i^A and \vec{b}_j^B in the projectile and in the target, respectively. We write this integration symbolically as

$$\int dT_{AB} := \int \prod_{i=1}^A d^2 b_i^A T_A(b_i^A) \prod_{j=1}^B d^2 b_j^B T_B(b_j^B) \quad (14)$$

with A and B being the nuclear mass numbers and with the so-called nuclear thickness function $T_A(b)$ being defined as the integral over the nuclear density $\rho_{A(B)}$:

$$T_A(b) := \int dz \rho_A(b_x, b_y, z). \quad (15)$$

It is convenient to use the transverse distance b_k between the two nucleons from the k th nucleon–nucleon pair, i.e.

$$b_k = |\vec{b}_0 + \vec{b}_{\pi(k)}^A - \vec{b}_{\tau(k)}^B|$$

where the functions $\pi(k)$ and $\tau(k)$ refer to the projectile and the target nucleons participating in the k th interaction (pair k). In order to simplify the notation, we define a vector b whose components are the overall impact parameter b_0 as well as the transverse distances b_1, \dots, b_{AB} of the nucleon pairs:

$$b = \{b_0, b_1, \dots, b_{AB}\}.$$

Then the nucleus–nucleus interaction cross section can be obtained by applying the cutting procedure to the elastic scattering diagram and written in the form

$$\sigma_{\text{inel}}^{AB}(s) = \int d^2 b_0 \int dT_{AB} \gamma_{AB}(s, b) \quad (16)$$

where the so-called nuclear profile function γ_{AB} represents an interaction for given transverse coordinates of the nucleons.

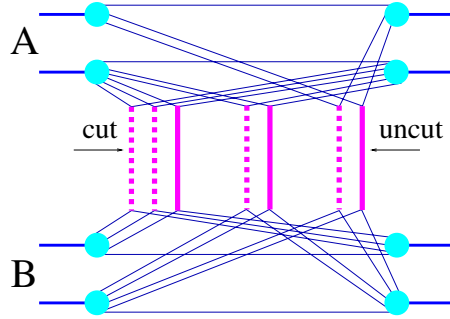


Figure 10. Example for a cut multiple scattering diagram, with cut (broken lines) and uncut (full lines) elementary diagrams. This diagram can be translated directly into a formula for the inelastic cross section (see text).

The calculation of the profile function γ_{AB} as the sum over all cut diagrams of the type shown in figure 10 does not differ from the hadron–hadron case and follows the rules formulated in the preceding section and listed as follows.

- For a remnant carrying the light cone momentum fraction x (x^+ in case of projectile, or x^- in case of target), one has a factor $F_{\text{remn}}(x)$.
- For each cut elementary diagram (a real elementary interaction is represented in figure 10 as a dashed vertical line) attached to two participants with light cone momentum fractions x^+ and x^- , one has a factor $G(x^+, x^-, s, b)$. Apart from x^+ and x^- , G is also a function of the total squared energy s and of the relative transverse distance b between the two corresponding nucleons (we use G as an abbreviation for G_{IP}^{NN} for nucleon–nucleon scattering).
- For each uncut elementary diagram (a virtual emission is represented in figure 10 as a vertical line) attached to two participants with light cone momentum fractions x^+ and x^- , one has a factor $-G(x^+, x^-, s, b)$, with the same G as used for the cut diagrams.
- Finally, one sums over all possible numbers of cut and uncut Pomerons and integrates over the light cone momentum fractions.

So we find

$$\begin{aligned} \gamma_{AB}(s, b) = & \sum_{m_1 l_1} \dots \sum_{m_{AB} l_{AB}} (1 - \delta_{0 \sum m_k}) \int \prod_{k=1}^{AB} \left\{ \prod_{\mu=1}^{m_k} dx_{k,\mu}^+ dx_{k,\mu}^- \prod_{\lambda=1}^{l_k} d\tilde{x}_{k,\lambda}^+ d\tilde{x}_{k,\lambda}^- \right\} \\ & \times \prod_{k=1}^{AB} \left\{ \frac{1}{m_k!} \frac{1}{l_k!} \prod_{\mu=1}^{m_k} G(x_{k,\mu}^+, x_{k,\mu}^-, s, b_k) \prod_{\lambda=1}^{l_k} -G(\tilde{x}_{k,\lambda}^+, \tilde{x}_{k,\lambda}^-, s, b_k) \right\} \\ & \times \prod_{i=1}^A F_{\text{remn}} \left(x_i^+ - \sum_{\pi(k)=i} \tilde{x}_{k,\lambda}^+ \right) \prod_{j=1}^B F_{\text{remn}} \left(x_j^- - \sum_{\tau(k)=j} \tilde{x}_{k,\lambda}^- \right) \end{aligned} \quad (17)$$

with

$$x_i^{\text{proj}} = 1 - \sum_{\pi(k)=i} x_{k,\mu}^+ \quad x_j^{\text{targ}} = 1 - \sum_{\tau(k)=j} x_{k,\mu}^-$$

The summation indices m_k refer to the number of cut elementary diagrams and l_k to the number of uncut elementary diagrams, related to nucleon pair k . For each possible pair k (we have

altogether AB pairs), we allow any number of cut and uncut diagrams. The integration variables $x_{k,\mu}^\pm$ refer to the μ th elementary interaction of the k th pair for the cut elementary diagrams, the variables $\tilde{x}_{k,\lambda}^\pm$ refer to the corresponding uncut elementary diagrams. The arguments of the remnant functions F_{remn} are the remnant light cone momentum fractions, i.e. unity minus the momentum fractions of all the corresponding elementary contributions (cut and uncut). We also introduce the variables x_i^{proj} and x_j^{targ} , defined as unity minus the momentum fractions of all the corresponding cut contributions, in order to integrate over the uncut contributions (see below).

The expression for γ_{AB} sums up all possible numbers of cut Pomerons m_k with one exception due to the factor $(1 - \delta_{0\Sigma m_k})$: we do not consider the case of all m_k 's being zero, which corresponds to ‘no interaction’ and therefore does not contribute to the inelastic cross section. We may therefore define a quantity $\bar{\gamma}_{AB}$, representing ‘no interaction’, by taking the expression for γ_{AB} with $(1 - \delta_{0\Sigma m_k})$ replaced by $(\delta_{0\Sigma m_k})$:

$$\begin{aligned} \bar{\gamma}_{AB}(s, b) = & \sum_{l_1} \dots \sum_{l_{AB}} \int \prod_{k=1}^{AB} \left\{ \prod_{\lambda=1}^{l_k} d\tilde{x}_{k,\lambda}^+ d\tilde{x}_{k,\lambda}^- \right\} \prod_{k=1}^{AB} \left\{ \frac{1}{l_k!} \prod_{\lambda=1}^{l_k} -G(\tilde{x}_{k,\lambda}^+, \tilde{x}_{k,\lambda}^-, s, b_k) \right\} \\ & \times \prod_{i=1}^A F^+ \left(1 - \sum_{\pi(k)=i} \tilde{x}_{k,\lambda}^+ \right) \prod_{j=1}^B F^- \left(1 - \sum_{\tau(k)=j} \tilde{x}_{k,\lambda}^- \right). \end{aligned} \quad (18)$$

One may now consider the sum of ‘interaction’ and ‘no interaction’, and one easily obtains

$$\gamma_{AB}(s, b) + \bar{\gamma}_{AB}(s, b) = 1. \quad (19)$$

Based on this important result, we consider γ_{AB} to be the probability of having an interaction and correspondingly $\bar{\gamma}_{AB}$ to be the probability of no interaction for a fixed energy, impact parameter and nuclear configuration that is specified by the transverse distances b_k between nucleons, and we refer to equation (19) as the ‘unitarity relation’. However, we want to go even further and use an expansion of γ_{AB} in order to obtain probability distributions for individual processes, which then serves as a basis for the calculations of exclusive quantities.

The expansion of γ_{AB} in terms of cut and uncut Pomerons as given above represents a sum of a large number of positive and negative terms, including all kinds of interferences, which excludes any probabilistic interpretation. We have therefore to perform summations of interference contributions—summed over any number of virtual elementary scatterings (uncut Pomerons)—for given non-interfering classes of diagrams with given numbers of real scatterings (cut Pomerons) [20]. Let us write the formulae explicitly. We have

$$\begin{aligned} \gamma_{AB}(s, b) = & \sum_{m_1} \dots \sum_{m_{AB}} (1 - \delta_{0\Sigma m_k}) \int \prod_{k=1}^{AB} \left\{ \prod_{\mu=1}^{m_k} dx_{k,\mu}^+ dx_{k,\mu}^- \right\} \\ & \times \prod_{k=1}^{AB} \left\{ \frac{1}{m_k!} \prod_{\mu=1}^{m_k} G(x_{k,\mu}^+, x_{k,\mu}^-, s, b_k) \right\} \Phi_{AB}(x^{\text{proj}}, x^{\text{targ}}, s, b) \end{aligned} \quad (20)$$

where the function Φ representing the sum over virtual emissions (uncut Pomerons) is given by the following expression:

$$\begin{aligned} \Phi_{AB}(x^{\text{proj}}, x^{\text{targ}}, s, b) = & \sum_{l_1} \dots \sum_{l_{AB}} \int \prod_{k=1}^{AB} \left\{ \prod_{\lambda=1}^{l_k} d\tilde{x}_{k,\lambda}^+ d\tilde{x}_{k,\lambda}^- \right\} \prod_{k=1}^{AB} \left\{ \frac{1}{l_k!} \prod_{\lambda=1}^{l_k} -G(\tilde{x}_{k,\lambda}^+, \tilde{x}_{k,\lambda}^-, s, b_k) \right\} \\ & \times \prod_{i=1}^A F_{\text{remn}} \left(x_i^{\text{proj}} - \sum_{\pi(k)=i} \tilde{x}_{k,\lambda}^+ \right) \prod_{j=1}^B F_{\text{remn}} \left(x_j^{\text{targ}} - \sum_{\tau(k)=j} \tilde{x}_{k,\lambda}^- \right). \end{aligned} \quad (21)$$

This summation has to be carried out, before we may use the expansion of γ_{AB} to obtain probability distributions. This is far from trivial, the necessary methods are described in [10]. To make the notation more compact, we define matrices X^+ and X^- , as well as a vector m , via

$$X^+ = \{x_{k,\mu}^+\} \quad X^- = \{x_{k,\mu}^-\} \quad m = \{m_k\}$$

which leads to

$$\gamma_{AB}(s, b) = \sum_m (1 - \delta_{0m}) \int dX^+ dX^- \Omega_{AB}^{(s,b)}(m, X^+, X^-)$$

$$\bar{\gamma}_{AB}(s, b) = \Omega_{AB}^{(s,b)}(0, 0, 0)$$

with

$$\Omega_{AB}^{(s,b)}(m, X^+, X^-) = \prod_{k=1}^{AB} \left\{ \frac{1}{m_k!} \prod_{\mu=1}^{m_k} G(x_{k,\mu}^+, x_{k,\mu}^-, s, b_k) \right\} \Phi_{AB}(x^{\text{proj}}, x^{\text{targ}}, s, b).$$

This allows us to rewrite the unitarity relation, equation (19), in the following form:

$$\sum_m \int dX^+ dX^- \Omega_{AB}^{(s,b)}(m, X^+, X^-) = 1.$$

This equation is of fundamental importance, because it allows us to interpret $\Omega^{(s,b)}(m, X^+, X^-)$ as the probability density of having an interaction configuration characterized by m , with the light cone momentum fractions of the Pomerons being given by X^+ and X^- .

7. Virtual emissions and Markov chain techniques

What did we achieve so far? We have formulated a well defined model, introduced using the language of field theory, and in this way solving the severe consistency problems of the most popular current approaches. To proceed further, one needs to solve two fundamental problems:

- the sum Φ_{AB} over virtual emissions has to be performed,
- tools have to be developed to deal with the multidimensional probability distribution $\Omega_{AB}^{(s,b)}$.

Both tasks being very difficult. Introducing new numerical techniques, we were able to solve both problems, as discussed in detail in [10].

Calculating the sum over virtual emissions (Φ_{AB}) is achieved by parametrizing the functions G as analytical functions and performing analytical calculations. By studying the properties of Φ_{AB} , we find that at very high energies the theory is no longer unitary without taking into account screening corrections due to triple Pomeron interactions. In this sense, we consider our work as a first step to constructing a consistent model for high-energy nuclear scattering, but there is still work to be done.

Concerning the multidimensional probability distribution $\Omega_{AB}^{(s,b)}(m, X^+, X^-)$, we employ methods well known in statistical physics (Markov chain techniques). So finally, we are able to calculate the probability distribution $\Omega_{AB}^{(s,b)}(m, X^+, X^-)$, and are able to generate (in a Monte Carlo fashion) configurations (m, X^+, X^-) according to this probability distribution.

8. Summary

What are finally the principal features of our basic results, summarized in equations (16), (20) and (21)? In contrast to the traditional treatment (Gribov–Regge approach or parton model), all individual elementary contributions G depend explicitly on the light cone momenta of the elementary interactions, with the total energy–momentum being precisely conserved. Another very important feature is the explicit dependence of the screening contribution Φ_{AB} (the contribution of virtual emissions) on the remnant momenta. The direct consequence of properly taking into account the energy–momentum conservation in the multiple scattering process is the validity of the so-called AGK cancellations in hadron–hadron and nucleus–nucleus collisions in the entire kinematical region.

The formulae (16), (20) and (21) allowed us to develop a consistent scheme to simulate high-energy nucleus–nucleus interactions. The corresponding Monte Carlo procedure is exactly based on the cross section formulae so that the entire model is fully self-consistent.

References

- [1] Kaidalov A B and Ter-Martirosyan K A 1974 *Nucl. Phys. B* **75** 471
- [2] Werner K 1993 *Phys. Rep.* **232** 87
- [3] Capella A, Sukhatme U, Tan C-I and Tran Thanh Van J 1994 *Phys. Rep.* **236** 225
- [4] Gribov V N 1968 *Sov. Phys.–JETP* **26** 414
- [5] Gribov V N 1969 *Sov. Phys.–JETP* **29** 483
- [6] Sjostrand T and van Zijl M 1987 *Phys. Rev. D* **36** 2019
- [7] Wang X-N 1997 *Phys. Rep.* **280** 287
Wang X-N 1996 *Preprint* hep-ph/9605214
- [8] Abramovskii V A and Leptoukh G G 1992 *Sov. J. Nucl. Phys.* **55** 903
- [9] Braun M 1990 *Yad. Fiz.* **52** 257 (in Russian)
- [10] Drescher H J, Hladik M, Ostapchenko S, Pierog T and Werner K 2001 *Phys. Rep.* hep-ph/0007198 to be published
- [11] Amati D, Stanghellini A and Fubini S 1962 *Nuovo Cimento* **26** 896
- [12] Altarelli G 1982 *Phys. Rep.* **81** 1
- [13] Reya E 1981 *Phys. Rep.* **69** 195
- [14] Altarelli G and Parisi G 1977 *Nucl. Phys. B* **126** 298
- [15] Lipatov L N 1986 *Sov. Phys.–JETP* **63** 904
- [16] Ryskin M G and Shabelski Y M 1992 *Yad. Fiz.* **55** 2149 (in Russian)
- [17] Donnachie A and Landshoff P 1994 *Phys. Lett. B* **332** 433
- [18] Baker M and Ter-Martirosyan K A 1976 *Phys. Rep.* **28** 1
- [19] Glauber R J 1959 *Lectures on Theoretical Physics* (New York: Interscience)
- [20] Abramovskii V A, Gribov V N and Kancheli O V 1974 *Sov. J. Nucl. Phys.* **18** 308